Journal of Marine Science and Technology

Volume 22 | Issue 6 Article 2

RESEARCH ON SEALING PERFORMANCE OF HYDROSTATIC PRESSURE MECHANICAL SEAL

Wei-Bing Zhu
School of Mechanical Engineering and Automation, Xihua University, Chengdu, Sichuan, P. R. China.,
qazzwb@sohu.com

He-Shun Wang
School of Mechanical Engineering and Automation, Xihua University, Chengdu, Sichuan, P. R. China.

Sheng-Ren Zhou
School of Mechanical Engineering and Automation, Xihua University, Chengdu, Sichuan, P. R. China.

RESEARCH ON SEALING PERFORMANCE OF HYDROSTATIC PRESSURE MECHANICAL SEAL

Acknowledgements

This work was supported by the National Nature Science Foundation of China (Grant No. 51005188), the Training Fund of Sichuan Academic and Technical Leader (Grant No. 13202625), the Parental Affection Plan Project, China's Ministry of Education (Grant No. Z2014072), and the Xihua University Young Scholars Training Program (No. 01201415).

Journal of Marine Science and Technology, Vol. 22, No. 6, pp. 673-679 (2014)
DOI: 10.6119/JMST-014-0321-1

RESEARCH ON SEALING PERFORMANCE OF HYDROSTATIC PRESSURE MECHANICAL SEAL

Wei-Bing Zhu, He-Shun Wang, and Sheng-Ren Zhou

Key words: hydrostatic pressure mechanical seal, end face flow field, gas film stiffness, orifice compensation, finite element method.

ABSTRACT

The hydrostatic pressure mechanical seal has many advantages, and it can be used in rotating machines with lower speed. Based on the externally pressurized stable gas lubrication theory, the control equation of end face flow field for hydrostatic pressure mechanical seal with orifice compensation was established. The functional extremum algorithm and the finite element method were used to solve this equation. The effects of gas film thickness, air supply pressure, throttle orifice number and diameter, on face opening force and gas film stiffness were discussed in detail. The results show that the opening force decreases with the widening of face clearance and increases with the rising of air supply pressure. The gas film stiffness increases with the decreasing of the throttle orifice diameter, and increases with the reducing of the throttle orifice number.

I. INTRODUCTION

The dry gas seal has been used more frequently than rotating mechanical dynamic seal because of its advantages in low leak, environmental protection, energy saving, and long lifetime. Its stability, both in theoretical analysis and practice, primarily depends on the rotating speed of a unit [1, 3, 7, 10, 11]. The dry gas seal requires a small clearance for non-contacting rotation. When the rotating speed is high enough, this small clearance can be formed. Otherwise, the sealing property will drop, and the seal may even fail. In general, the rotating speed of the principal axis of a centrifugal compressor is very high, about 10000 rpm, so the dry gas seal can be used successfully in this type of equipment. As for machines with lower rotating speed, such as reaction kettle, it is difficult to form adequate gas film to reach the required opening force and stiffness, so the dry gas seal can not work normally. Yu [12] and Liu [4] made use of the theory of externally pressurized gas lubrication bearing to design a new-style of hydrostatic pressure mechanical seal which does not depend on the rotating speed of a unit. Its working principle is to form the end face stable gas film and the high opening force by the externally pressurized gas, then to make the non-contacting running. It is a new-style of mechanical seal which has an externally and internally pressurized structure. The externally pressurized structure (Fig. 1) has the advantages of stable seal performance and high reliability, good gas film stiffness, independent of sealing speed, and the ability to start heavy equipments under the complete gas-film lubrication conditions. Its disadvantages are static pressure gas provided by external gas source equipment, complex structure, and processing difficulties. Because the hydrostatic pressure mechanical seal has the advantages of environmental protection, energy saving, long lifetime, high efficiency and low maintenance cost, it has been widely used in petroleum, chemical and other industries.

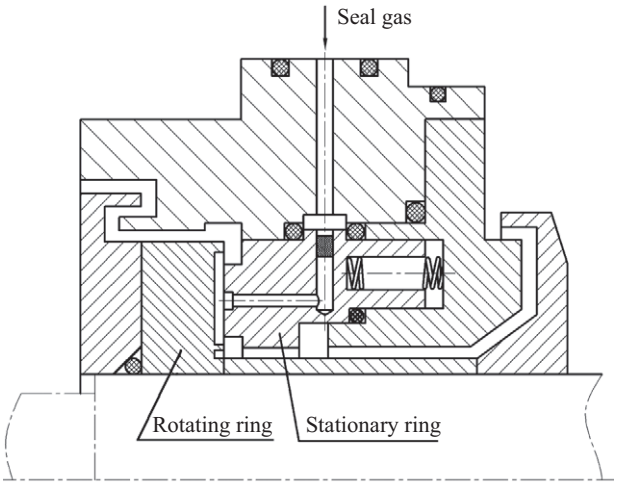

Fig. 1. Externally pressurized hydrostatic mechanical seal.

One of normal working conditions of the hydrostatic pressure mechanical seal is the stable gas film stiffness which is affected by many factors, such as grooved length, width of

Paper submitted 04/11/13; revised 12/30/13; accepted 03/21/14. Author for correspondence: Wei-Bing Zhu (e-mail: qazzwb@sohu.com).
School of Mechanical Engineering and Automation, Xihua University, Chengdu, Sichuan, P. R. China.

stationary ring end face, roughness of rotating and stationary ring end faces, sealing medium, end face clearance, and orifice compensation property. Tadashi Koga [8, 9] studied the seal performance of externally pressurized non-contacting mechanical seal and its application in extreme conditions, and discussed the end face pressure distribution, end face opening force, gas film stiffness and balance of forces in detail. Zhu [15] studied the performance of externally pressurized dry gas seal. In practical application, the gas agitated heat in the sealed chamber and the dissipated power due to viscous friction in the sealing interface will lead to a temperature rise on the rotating and stationary rings. Excessive high temperature and large temperature gradient will result in thermal deformation of the rotating and stationary rings, point contacting between end faces, leakage increasing, and unstable gas film. All these problems will seriously affect the performance, running safety and seal lifetime. Zhu [14, 16] calculated the amount of heat generation and the thermal deformation of externally pressurized hydrostatic mechanical seal, and discussed the effects of material and structural parameters on the axial and radial thermal deformations, as well as on the deformation taper of end faces, and then optimized the rotating and stationary rings [13]. Liu [5] and Dang [2] studied the gas lubrication technology systematically. Yu [12] researched the effects of groove length ratio, groove width ratio, groove depth, throttle orifice diameter, face roughness and face clearance on the sealing performance of externally pressurized hydrostatic mechanical seal. Yu did not consider the effect of throttle orifice characteristics, so his conclusions can not match the actual situation. In fact, the characteristics of throttle orifice including air supply pressure, number and diameter, distribution and outlet pressure, will directly affect the face opening force and the stability of gas film stiffness. The characteristic of throttle orifice is an important factor that affects gas film stability and continuity. In this paper, according to the theory of externally pressurized stable gas lubrication, the externally pressurized hydrostatic mechanical seal with orifice compensation was studied. The effects of gas film thickness, air supply pressure, throttle orifice distribution, number and diameter on the face opening force and the gas film stiffness were discussed in detail. All these will provide theoretical bases for the optimal design of pressurized hydrostatic mechanical seal.

II. MODEL OF FACE FLOW FIELD AND ITS BOUNDARY CONDITIONS

To simplify the model, the following assumptions were made:

(1) $K_n = \lambda/h < 0.01$, where K_n is the Knudsen number, λ is the mean free path of gas molecules, and h is the gas film thickness. And the lubrication gas is a continuous flow medium.
(2) The lubrication gas is a kind of Newtonian fluids with a laminar movement, that is to say, the shear stress is proportional to the velocity gradient.
(3) Along the direction of the gas film thickness, there is no change in pressure, $\frac{\partial P}{\partial y} = 0$.
(4) Compared with the viscous shearing stress, the inertial force of the fluid is small and negligible, $\frac{du}{dt} = \frac{dv}{dt} = \frac{dw}{dt} = 0$.
(5) The volume force of the lubrication gas is not considered.
(6) The velocity of fluid quality points attaching to the solid interface is equal to that on the solid interface.
(7) The effect of the end face morphology is ignored. There is a gas film between the end faces, so the two sealing surfaces will not contact with each other. The thickness of the gas film is h, and it is the same everywhere in areas without grooves.
(8) The direction of gas film thickness is taken as the y axis, and the expanded gas lubricated surfaces are taken as the plane of x and z axes. The airflow velocity component v along y axis is much smaller than the velocity components u and w along x and z axes. Comparing with the velocity gradients $\frac{\partial u}{\partial y}$ and $\frac{\partial w}{\partial y}$, other velocity gradients can be neglected.
(9) The neutrality of sealing is good, so the effect of system disturbance and vibration on the gas film flow field can be neglected during the working process.

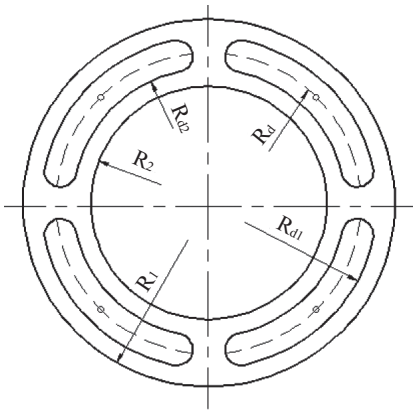

Fig. 2. End face structure of stationary ring.

The shallow grooves machined on the end face of stationary ring were compensation slots. The throttle orifice machined at the center of the shallow groove was the channel for externally pressurized gas (Fig. 2). Generally, the externally pressurized hydrostatic mechanical seal adopts orifice compensation, so the flow field model of the faces can use the Reynolds equation for externally pressurized stable gas lubrication [6],

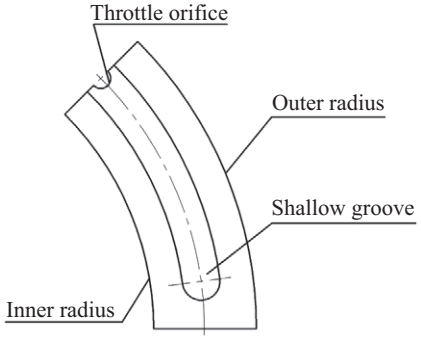

Fig. 3. Computational domain.

$$\frac{\partial}{\partial x}\left(h^3\frac{\partial f}{\partial x}\right)+\frac{\partial}{\partial z}\left(h^3\frac{\partial f}{\partial z}\right)=0 \tag{1}$$

where f is the square of gas pressure, $f = P^2(x, z)$; and h is the thickness of gas film, $h = h(x, z)$.

In a continuous gas flow field, the pressure and flow rate will change abruptly at the throttle orifice, so it will be difficult to meet the boundary conditions and to solve the equation. Furthermore, the flow rate boundary conditions of the throttle orifice will affect the solution precision. In this paper, the flow rate of throttle orifice was added to the conventional Reynolds equation, so the equation expressed in cylindrical coordinates for externally pressurized hydrostatic mechanical seal with orifice compensation can be written as

$$\frac{1}{r}\frac{\partial}{\partial r}\left(rh^3\frac{\partial f}{\partial r}\right)+\frac{1}{r^2}\frac{\partial}{\partial\theta}\left(h^3\frac{\partial f}{\partial\theta}\right)+Q\delta=0 \tag{2}$$

where $Q\delta$ is the flow rate of throttle orifice, $Q = 24\eta P_a\rho v/\rho_a$; P_a is the atmospheric pressure; ρ_a is the gas density; ρ is the density of gas flowing through the throttle orifice; v is the velocity of gas flowing through the throttle orifice; η is the viscosity of lubrication gas; and δ is the Dirac delta function, at the throttle orifice, $\delta = 1$, otherwise, $\delta = 0$.

Taking $\xi = \ln r$, Eq. (2) can be simplified with the method of variable transformation,

$$\frac{\partial}{\partial\xi}\left(h^3\frac{\partial f}{\partial\xi}\right)+\frac{\partial}{\partial\theta}\left(h^3\frac{\partial f}{\partial\theta}\right)+r^2Q\delta=0 \tag{3}$$

As shown in Fig. 3, in the computational domain, there is a symmetrical boundary, an environmental atmospheric boundary, and a throttle orifice boundary. In order to solve Eq. (3), the boundary conditions of pressure and throttle orifice must be satisfied. At the environmental atmospheric boundary, $P = P_a$; at the symmetrical boundary, $\partial P/\partial n = 0$; and at the throttle orifice boundary, $P = P_{di}$.

Where P_{di} is the outlet pressure of throttle orifice, $i = 1, 2, \ldots NL$; NL is the number of throttle orifice; and n is the normal direction of symmetrical boundary.

Usually all the throttle orifices are not connected to each other, so the throttle orifice boundary refers to the sum of all throttle boundaries. The pressure of throttle orifice boundary is unknown. By synchronously solving Eq. (3) and the flow rate equation of the throttle orifice, the boundary pressure of the throttle orifice can be obtained. The flow rate equation of the throttle orifice is,

$$m_i = AP_0\Phi(2\rho_a/P_a)^{1/2}\psi \tag{4}$$

$$\psi=\begin{cases}\left[\dfrac{k}{2}\left(\dfrac{2}{k+1}\right)^{(k+1)/(k-1)}\right]^{1/2} & \left(\dfrac{P_{di}}{P_0}\le\beta_0\right)\\ \left\{\dfrac{k}{k-1}\left[\left(\dfrac{P_{di}}{P_0}\right)^{2/k}-\left(\dfrac{P_{di}}{P_0}\right)^{(k+1)/k}\right]\right\}^{1/2} & \left(\dfrac{P_{di}}{P_0}>\beta_0\right)\end{cases} \tag{5}$$

where m_i is the mass flowing out of the throttle orifice, A is the area of the throttle orifice, P_0 is the air supply pressure, Φ is the discharge coefficient, ψ is the discharge function, $\beta_0 - (2/(k + 1))^{k/(k-1)}$, and k is the ratio of heat insulation, as for air, $k = 1.4$.

III. SOLUTION OF REYNOLDS EQUATION

Eq. (3) is a second order partial differential equation, and we can use the finite difference method and the finite element method to solve it. The finite element method can adapt to various complicated boundaries and has heterogeneous mesh generation. So, in this paper, the finite element method and the functional extremum algorithm were used to solve Eq. (3). At first, Eq. (3) was transformed into a special problem of functional extremum [5]. By making use of the variation principle and taking $f(\xi, \theta)$ as an independent variable, a function can be constructed,

$$\Phi(f(\xi,\theta))=\int_\Omega\frac{h^3}{2}\left[\left(\frac{\partial f(\xi,\theta)}{\partial\xi}\right)^2+\left(\frac{\partial f(\xi,\theta)}{\partial\theta}\right)^2\right]d\xi d\theta$$
$$-\int_\Omega r^2Qf(\xi,\theta)\delta d\xi d\theta \tag{6}$$

From Eq. (6), we can get that various different pressure distributions have their corresponding functions $\Phi(f(\xi, \theta))$, and only one of them can obtain the extremum of the function $\Phi(f(\xi, \theta))$. An equation set with N unknown numbers can be obtained by finding the partial derivative of the function $\Phi(f(\xi, \theta))$ and letting it to be zero. Then the finite element method with three node triangle elements was used to solve this equation set. The pressure square of an arbitrary point within the triangle element can be expressed as a function of

the pressure square of all three nodes, and its corresponding interpolating function is

$$f = N_j f_j + N_l f_l + N_m f_m \tag{7}$$

where f_j, f_l, f_m are the pressure squares of each node, N_j, N_l, N_m are the shape functions of each node, and j, l, m are the numbers of each node respectively.

The integral of Eq. (6) can be expressed as the integral sum of each finite element,

$$\Phi(f(\xi,\theta)) - \sum_e \frac{1}{2}\int_{A_e} h^3 \left[\left(\frac{(\partial f(\xi,\theta))}{\partial \xi} \right)^2 + \left(\frac{(\partial f(\xi,\theta))}{\partial \theta} \right)^2 \right] d\xi d\theta$$

$$- \sum_e \int_{A_e} r^2 Q f(\xi,\theta) d\xi d\theta \delta \tag{8}$$

Substituting Eq. (7) into Eq. (8), an algebraic equation set with nonlinear characteristics can be obtained,

$$KF = T \tag{9}$$

where F is the vector of node pressure, $F = [f_1, f_2, \ldots, f_N]^{\mathrm{T}}$, $T = [t_1, t_2, \ldots, t_N]^{\mathrm{T}}$, K is the stiffness matrix, and N is the number of node.

T is a nonlinear column matrix having a relation with the known boundary pressure and the outlet pressure of the throttle orifice P_{di}. When the node j corresponds with the node of the throttle orifice,

$$t_j = k_1 u_i m_i \delta \tag{10}$$

where $k_1 = 24\eta P_a/\rho_a$, u_i is the ratio of the throttle orifice area within the computational domain to the whole area of the throttle orifice.

In Eq. (9), in addition to the unknown pressure square F, the flow rate item m_i which is included in T is also unknown, and m_i is the nonlinear function of the node pressure P_{di}. The successive overrelaxation method and the proportional partition method were used to solve Eq. (9). After obtaining the node pressure, the face opening force and the stiffness of the sealing ring can be obtained. The calculating procedures are:

Step 1. An initial value is taken as the outlet pressure of the throttle orifice for the first loop calculation $f_{di}^{(1)} = (1, 2, \ldots, NL)$, and $f_{di}^{(1)}$ are elements of matrix $F^{(1)}$. By using Eq. (4) and Eq. (10), the values of m_i and t_j can be obtained at the same time, and then other elements in column matrix T can be determined. In matrix T, except those elements containing m_i, other elements are zero or have a known quantity.

Step 2. According to matrixes T and K, the successive overrelaxation method is used to solve Eq. (9). The first approximation of node pressure $F^{(1)*}$ and the pressure function of throttle orifice $f_{di}^{(1)*} = (1, 2, \ldots, NL)$ can be obtained.

And then, Eq. (11) is used to determine whether this calculation can meet the required precision.

$$\left| \frac{f_{di}^{(1)*} - f_{di}^{(1)}}{f_{di}^{(1)}} \right| < \varepsilon \tag{11}$$

where ε is the required precision.

If Eq. (11) is satisfied, then end the iterative calculation. Otherwise, the initial value for the next loop calculation is determined by using the proportional partition method and according to Eq. (12). The above calculating procedures will be repeated until Eq. (11) is satisfied.

$$f_{di}^{(s+1)} = f_{di}^{(s)} + \frac{1}{G\alpha}(f_{di}^{(s)*} - f_{di}^{(s)}) \tag{12}$$

where s is the loop index, G is the proportional partition factor, and α is the adjusting factor.

According to the pressure distribution of face nodes, the opening force for each element, F_e can be obtained. Hence the whole face opening force and the gas film stiffness can be obtained,

$$F = \sum_e F_e \quad K = \Delta F / \Delta h \tag{13}$$

where F is the opening force on the whole face, K is the gas film stiffness on the face, ΔF is the variable of face opening force, and Δh is the variable of gas film thickness.

IV. MODEL VALIDATION

At present, little work has been done on the externally pressurized hydrostatic mechanical seal, but many researchers have studied the externally pressurized gas lubrication bearing. We can use the researching results on externally pressurized gas lubrication thrust bearing to validate the model established in this paper.

In reference [5], the geometric parameters of thrust bearing are outer radius $R_1 = 60$ mm, inner radius $R_2 = 20$ mm, $NL = 12$, $d_r = 0.2$ mm, face clearance $h_0 = 0.0026$ mm, $P_0 = 0.4$ MPa, and $P_a = 0.1$ MPa. The carrying capacity of the thrust bearing obtained from the model established in this paper is 353.8 N, while in the reference, the carrying capacity is 353.6 N. The pressure distributions on the thrust bearing are shown in Fig. 4 and Fig. 5. It is obvious that these results are consistent, so the model established in this paper is accurate.

V. SEALING PERFORMANCE

By using the above theory and method, the hydrostatic

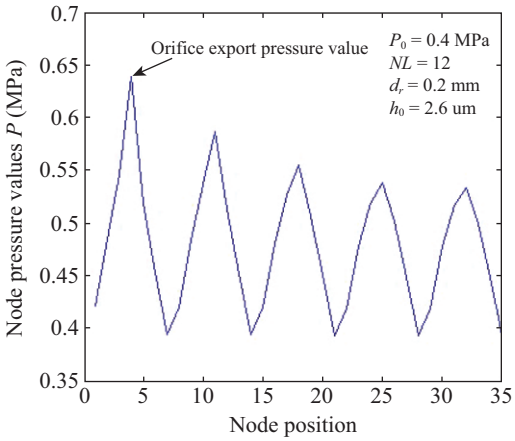

Fig. 4. Calculating results in this paper.

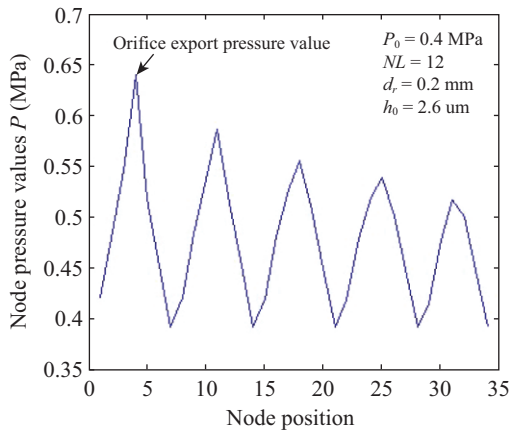

Fig. 5. Calculating results in the reference.

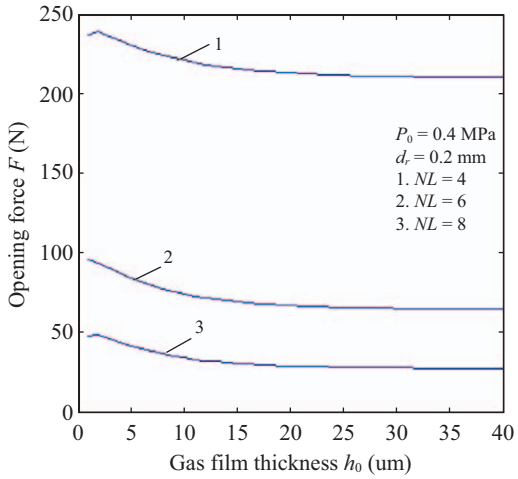

Fig. 6. Effect of throttle orifice on opening force.

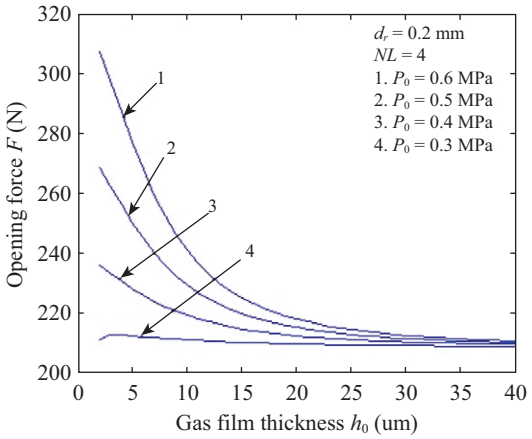

Fig. 7. Effect of air supply pressure on opening force.

pressure mechanical seal with orifice compensation can be numerically simulated. The main manipulation and structural parameters of externally pressurized hydrostatic mechanical seal in the experiment were P_a = 0.1 MPa; P_0 = 0.4 MPa, 0.5 MPa, 0.6 MPa; R_2 = 35.5 mm; R_1 = 47 mm; d_r = 0.1 mm, 0.15 mm, 0.2 mm, 0.25 mm; NL = 4, 6, 8; ρ_a = 1.23 kg/m^3; η = 1.84 × 10^{-5} Pa.s; and Φ = 0.8. By using the MATLAB software to program the finite element model, the face opening force, gas film stiffness and gas film pressure distribution can be obtained.

By taking the maximal opening force as the calculating criterion and the thickness of gas film as the design variable, the air supply pressure and the number of throttle orifice under different conditions were numerically simulated, as shown in Fig. 6 and Fig. 7. It can be seen that the face opening force decreases slowly with the widening of the face clearance, decreases quickly with the increasing of throttle orifice number, and increases with the rising of air supply pressure. In order to get a higher face opening force, the number of throttle orifice should be 4.

By taking the maximal gas film stiffness as the calculating criterion and the thickness of gas film as the design variable, the air supply pressure and the number of throttle orifice under different conditions were numerically simulated, as shown in Fig. 8. It can be seen that the gas film stiffness increases with the rising of air supply pressure. When the thickness of gas film is small, the increasing range of gas film stiffness is large. But with the increasing of gas film thickness, the increasing range of gas film stiffness gradually reduces and approaches to zero. When the numbers of throttle orifice are 2, 4, 6, or 8, the gas film stiffness reduces with the increasing of throttle orifice number. In order to get a higher gas film stiffness, the number of throttle orifice should be 4.

The effect of throttle orifice diameter on the gas film stiffness is shown in Fig. 9. When the thickness of gas film is small, the gas film stiffness increases with the decreasing of throttle orifice diameter. It is difficult to machine smaller throttle orifice. Furthermore, smaller throttle orifice will result in blockage, while bigger throttle orifice will reduce the gas film stiffness and increase the gas flow rate. So the diameter of throttle orifice should be controlled within 0.15~0.2 mm.

By taking the node pressure as the objective function and

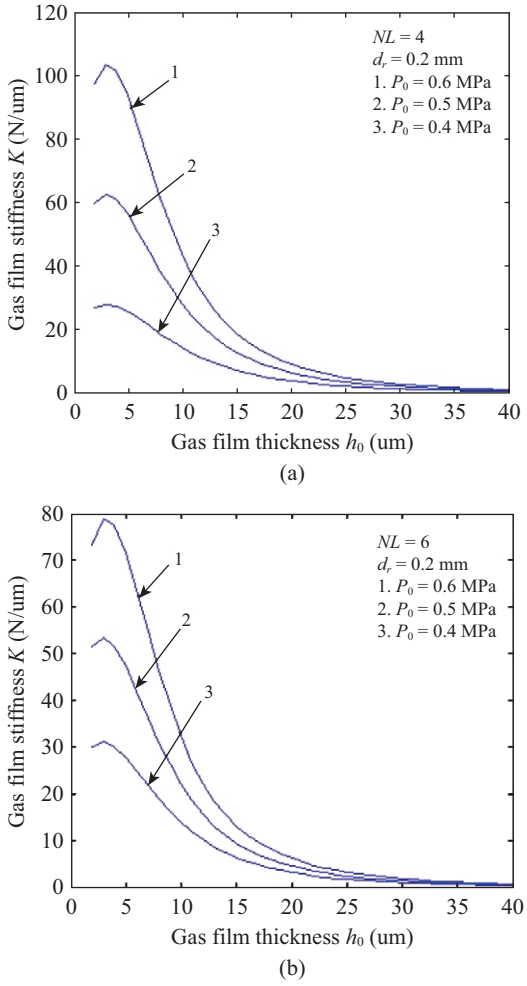

Fig. 8. Effect of throttle orifice number on gas film stiffness.

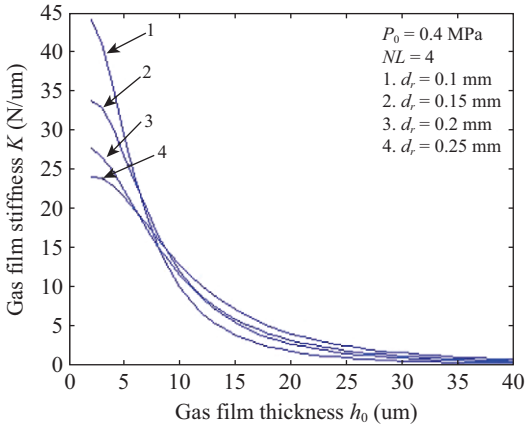

Fig. 9. Effect of throttle orifice diameter on gas film stiffness.

the node position as the variable, the node pressure distribution was calculated, as shown in Fig. 10. The pressure drops obviously when the seal gas flows through the throttle orifice. The maximum pressure (0.3578 MPa) occurs at the center of the throttle orifice, and the minimum pressure occurs at the

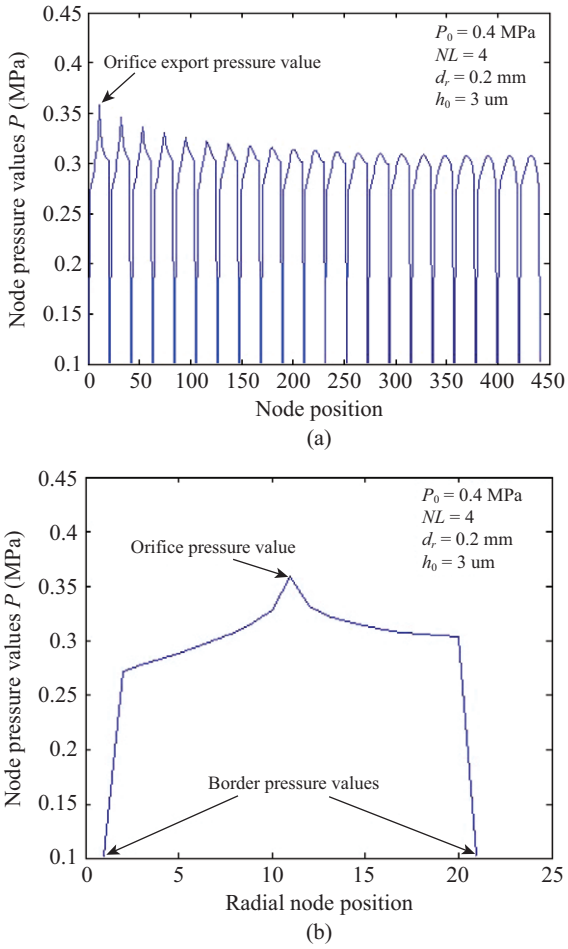

Fig. 10. Curve of node pressure distribution.

boundary between the outer radius and the inner radius. From the center to the boundary, the pressure drops gradually, and the pressure at the inner radius boundary is smaller than that at the outer radius boundary.

The optimized parameters for externally pressurized hydrostatic mechanical seal with orifice compensation can be obtained from the numerical simulation results. For example, the air supply pressure is 0.5 MPa, the throttle orifice diameter is 0.15 mm, the gas film thickness is 3 μm, and the number of throttle orifice is 4.

VI. CONCLUSION

Hydrostatic pressure mechanical seal has many advantages, and it can be used in machines with lower rotating speed, such as reaction kettle. Based on the externally pressurized stable gas lubrication theory and by adding the flow rate of throttle orifice to the conventionally stable externally pressurized gas lubrication equation, the Reynolds equation for the externally pressurized hydrostatic mechanical seal with orifice compensation is established, which is a second order partial differential equation.

The functional extremum algorithm and the finite element method are used to solve the equation. The researching results of externally pressurized gas lubrication thrust bearing are used to validate this model. The pressure distribution between the end faces and the opening force are obtained. The effects of gas film thickness, air supply pressure, number and diameter of throttle orifice, face opening force and gas film stiffness are discussed in detail.

The results show that the pressure drops obviously when the seal gas flows through the throttle orifice, and the pressure drop increases with the widening of face clearance. The opening force decreases with the widening of face clearance and increases with the rising of air pressure supply. Within a certain face clearance, a bigger gas film opening force and gas film stiffness can be obtained, so the non-contacting running can be realized. From the center to the boundary, the face pressure drops gradually. The gas film stiffness increases with the decreasing of throttle orifice diameter, and the gas film stiffness increases with the reducing of throttle orifice number. The optimized parameters for the hydrostatic pressure mechanical seal with orifice compensation can be obtained from the numerical simulation results. For example, the air supply pressure should be 0.5 MPa, the throttle orifice diameter should be 0.15 mm, the gas film thickness should be 3 μm, and the throttle orifice number should be 4.

ACKNOWLEDGMENT

This work was supported by the National Nature Science Foundation of China (Grant No. 51005188), the Training Fund of Sichuan Academic and Technical Leader (Grant No. 13202625), the Parental Affection Plan Project, China's Ministry of Education (Grant No. Z2014072), and the Xihua University Young Scholars Training Program (No. 01201415).

REFERENCES

1. Cai, J., Shi, J., Li, S., and Zhang, Q., "Study on air-liquid mixture mechanical seal phase transition radius and its influencing factors," *Lubrication Engineering*, Vol. 38, No. 6, pp. 12-16 (2013).
2. Dang, G., *Gas Lubrication Technology*, Southwest University Press, Nanjing, China (1990).
3. Fujiwara, S. and Fuse, T., "Advanced aerostatic dry gas seal," *16th International Conference on Fluid Sealing, BHR Group 2000 Fluid Sealing*, pp. 483-499 (2000).
4. Liu, F., *The Research of Aerostatic Gas Seal*, Master Thesis, Xihua University, Chengdu, China (2010).
5. Liu, T., Liu, Y., and Chen, S., *Externally Pressurized Gas Lubrication*, Harbin Institute of Technology Press, Harbin (1990).
6. Liu, T., Peng, C., and Ge, W., "On the discretization of orifice compensated externally pressurized lubrication and computational convergency," *Tribology*, Vol. 21, pp. 139-142 (2001).
7. Stolarski, T. A. and Xue, Y., "Performance study of a back-depression mechanical dry gas seal," *Proceedings of the Institution of Mechanical Engineers, Part J*, Vol. 212, pp. 279-290 (1998).
8. Tadashi, K. and Takuya, F., "High stiffness seal and its application to extreme condition," *Proceedings of the 10th International Conference on Fluid Sealing (Paper II)*, British Hydromechanics Research Assn Cranfield (1984).
9. Tadashi, K. and Takuya, F., "The hydrostatic gas noncontact seal," *ASLE Translations*, Vol. 29, pp. 505-514 (1985).
10. Wang, H., *Research on Working Stability of Dry Gas Seal*, Ph.D. Dissertation, Southwest Traffic University, Chengdu, China (2006).
11. Wang, J. and Zhang, G., "Study on nonlinear dynamic coefficients and transient vibration response for a non-contact mechanical seal," *China Mechanical Engineering*, Vol. 23, No. 6, pp. 642-646 (2012).
12. Yu, J., *Research on Characteristic of Aerostatic Gas Lubricating Mechanical Seal*, Master Thesis, Kunming University of Science and Technology, Kunming, China (2008).
13. Zhu, W., Wang, H., and Dong, L., "Influencing factors of thermal deformation on hydrostatic pressure mechanical seal and optimization of rotating and stationary ring," *TELKOMNIKA*, Vol. 11, No. 2, pp. 896-905 (2013).
14. Zhu, W., Zhou, S., and Wang, H., "End surface temperature field analysis on static pressure dry gas seal," *Journal of Xihua University (Natural Science Edition)*, Vol. 29, No. 6, pp. 1-3 (2010).
15. Zhu, W., Zhou, S., and Wang, H., "Performance of externally pressurized dry gas seal," *Advanced Materials Research*, Vols. 335-336, pp. 610-614 (2011).
16. Zhu, W., Zhou, S., and Wang, H., "Thermal deformation in a static pressure dry gas seal," *Applied Mechanics and Materials*, Vols. 217-219, pp. 2406-2409 (2012).